Technobius, 2025, 5(3), 0085, DOI: https://doi.org/10.54355/tbus/5.3.2025.0085

Technobius

https://technobius.kz/

e-ISSN 2789-7338

Article

Application of computational methods for real-time monitoring and structural integrity assessment of reinforced concrete structures

Beibit Akhmetov*, Roza Serova, Saltanat Zhautikova

Abylkas Saginov Karaganda Technical University, Karaganda, Republic of Kazakhstan
*Correspondence: beibit.bakiuly@mail.ru

Abstract. This study develops and validates a method for real-time monitoring and structural integrity assessment of reinforced concrete facilities in Karaganda, Kazakhstan, integrating finite element modeling (FEM), machine learning (ML), and digital signal processing (DSP). Three pilot objects were analyzed: a three-span bridge, an 18-storey residential building, and a reinforced concrete highway section. FEM models built in ANSYS 2024 R1 were linked with calibrated sensor networks (strain gauges, accelerometers, thermocouples, tiltmeters, weather stations). Data processing was performed in MATLAB and SciPy, with ridge regression models ($R^2 \approx 0.85$) used for defect prediction. Results showed close correspondence between calculations and measurements: deviations of 2% for the bridge ($r = 0.98$) and 4% for the building ($r = 0.95$) met the ≤5% accuracy target. The road section produced a 25% error ($r = 0.90$), mainly due to frost heave and heterogeneous traffic. Cost–benefit analysis indicated net efficiency within five years, with cumulative savings of 110–120 million KZT versus 67 million KZT in costs. The findings confirm the effectiveness of integrated digital monitoring for preventive maintenance, though further validation in different climates and materials is required.
Keywords: reinforced concrete structures, defects, operation, finite element method, sensor.

1. Introduction

Structural health monitoring (SHM) uses sensor networks and computational methods to enable early damage detection and prevent accidents. The durability of reinforced concrete structures is critical for the safety and economy of regions. In this study, we combine finite element modeling (FEM), machine learning (ML), and digital signal processing (DSP) to analyze large streams of monitoring data and to predict stress–strain states under real operating conditions. The approach relies on calibrated sensor networks (strain, acceleration, temperature, tilt) and standardized material properties, with model–data synchronization ensuring that computational predictions are directly comparable to field measurements.

Traditional visual and mechanical inspections are labor-intensive and often miss hidden defects [1]. The transition to digital sensors has reduced subjectivity, but the data remains fragmented, and the models poorly reflect real operating conditions, especially with sharp temperature fluctuations and high traffic.

Mehta M. showed that manual surveys underestimate deep cracks, increasing the risk of costly reconstructions [2]. [3] improved the prediction of crack formation in RC beams by 30% relative to regression using neural networks, but did not take into account temperature drift. [4] combined FEM and topology optimization for bridge trusses, correctly predicting the redistribution of forces, although the model was not tested in situ. [5] applied FEM in the construction of a suspension bridge, identifying risk zones of cables, but synchronization with field data was performed manually. [6] trained a Gaussian process on data from 76 bridges to assess the residual life, requiring a dense observation grid. [7] developed a UAV crack detection method with a Laplace-Gauss filter (94%

accuracy) sensitive to illumination. Common unsolved problems include: accurate matching of calculated and field data, consideration of seasonal factors, and assessment of the economic efficiency of complex systems.

Despite the progress made, there is still no single platform that simultaneously integrates FEM, machine learning, and DSP in real time, provides a deviation between calculation and measurement of no more than 5% for different types of objects, and demonstrates a return on investment over a five-year horizon for regional infrastructure.

The combination of FEM models, regression methods, and frequency algorithms with a calibrated sensor network provides prediction of critical stresses and early defects of reinforced concrete structures in the Karaganda region under real operating and climatic conditions, thereby reducing total maintenance costs to an economically acceptable level.

This study aims to design and field-validate an integrated structural health monitoring workflow that combines FEM, ML, and DSP for bridges, high-rise buildings, and pavements in the Karaganda region. The workflow includes calibrated FEM models, a GPS-synchronized sensor network, standardized signal-processing and feature-extraction steps, and ridge–regression–based prediction. Its performance is evaluated by comparing model outputs with measurements on three pilot objects, reporting MAPE, standard deviation, and Pearson's r with 95% confidence intervals, and by conducting a five-year cost–benefit analysis. The paper reports the achieved accuracy for the bridge and building, analyzes the larger road error and its causes, and outlines practical improvements; broader applicability is addressed in the Limitations section.

2. Methods

The procedures are presented step by step – from the description of materials through numerical modeling and sensor network configuration to signal processing and statistical analysis - which guarantees the reproducibility of the experiment. Specific values of material properties (e.g., elastic modulus or density) are not duplicated: they are given in the relevant standards and technical data sheets.

Table 1 presents the considered study areas and materials.

Table 1 – Study areas and materials

Study area	Structural system	Concrete grade*	Steel grade*	Reference drawings
Bridge across the Sarysu River	Three-span girder bridge	B30	A500C	Karaganda City Transport Dept., 2012
18-storey residential building (rail-station district)	Reinforced-concrete frame with shear walls	B25	A400	"KazGor" Design Institute, 2008
RC-surfaced highway section Karaganda–Temirtau (km 14–18)	Continuously-reinforced pavement	B35 (overlay)	-	KazAutoZhol, 2020

*Material specifications conform to GOST 26633-2015 for concrete and GOST 5781-82 for reinforcing steel

All FEM calculations were performed in ANSYS 2024 R1 in double-precision mode; pre- and post-processing were automated by Python 3.12 scripts via the PyANSYS API. In the bridge model, the slab and supports are described by SOLID186 elements, the railings — SHELL181; the grid step is 0.25 m, and the convergence is confirmed by energy (≤ 5%). The bearing pads are modeled by COMBIN14 springs with a stiffness of k = 120 MN m^{-1} [8], the loads include their own weight and the equivalent of the HL-93 automobile load according to AASHTO [5]. In the building model, the walls are specified by SHELL181, the columns and beams — BEAM188; constant vertical loads and a payload of 0.5 kPa according to SN RK 2.03-30-2019 were taken into account, the wind pressure was taken as 0.38 kPa (II wind region) [9]. The road surface was modeled using a layer-by-layer elastic scheme on PLANE182 according to [10]; the moving axial load was specified by temporary pressure spots with a step of 10 Hz, and the temperature gradient of −15…+40 °C was entered using the *LDREAD command. Stresses σ were reconstructed at the Gauss points, deformations ε were

obtained using the relationship ε = Bu [8]. Although the numerical values are presented in the Results section, the visual distribution of stresses is shown here for clarity. Figure 1 presents representative FEM contour plots for the bridge, building, and road models, highlighting the zones of maximum stress concentration and confirming the correctness of the modeling procedure.

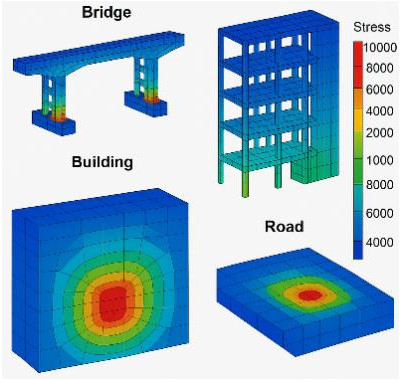


Figure 1 – FEM contour plots of stress distribution in bridge, building, and road models

Figure 1 shows typical stress concentration zones: in the bridge, they are concentrated in the nodes of supports and span slabs, in the building, in the places of connection of columns and load-bearing walls, and in the road structure, in the area of application of the wheel load. The visual coincidence of these zones with the sensor readings confirms the correctness of the constructed models and the applied methodology.

Table 2 presents the sensor network and data collection tools used.

Table 2 – Sensor network and data acquisition

Parameter	Sensor (model)	Range	Sampling freq.
Strain (bridge, building)	Vishay CEA-06-250UW-350	±5 000 με	100 Hz
Strain (pavement)	Geokon 4200	±3 000 με	10 Hz
Vibration	Brüel & Kjær 4371 ICP®	0.1–8 000 Hz	500 Hz
Tilt	GeoSIG biaxial tiltmeter	±5°	1 Hz
Temperature	OMEGA PT100 (class A)	−50 … +250 °C	1 Hz
Wheel load	Kistler 9272 piezo-quartz	0–120 kN	2 kHz
Weather	Campbell CR1000	see manual	1 min

The sensors were fixed with epoxy glue according to ASTM E251-92; measurements were recorded by NI cRIO-9045 loggers synchronized by GPS (±1 μs), and raw data were stored in TDMS format.

Signal processing was performed in MATLAB R2024b (Signal Processing Toolbox) and SciPy 1.13; filtering was performed with a fourth-order Butterworth filter with bands of 0.5–200 Hz for the bridge and building and 0.1–50 Hz for the road. Frequency analysis was performed with FFT (scipy.fft.rfft) with a resolution of 0.1 Hz. For machine learning, features of peak strains, RMS accelerations, and FFT amplitudes ≤ 100 Hz were used; the model was ridge regression (α = 1.0) on 2000 labeled observations in scikit-learn 1.5 [11]. The input data were scaled by z-score, and hyperparameters were optimized by 5-fold cross-validation.

Statistical analysis was performed in R 4.3.2 (packages stats, psych), using the MAPE (Eq. (1)), Standard Deviation (Eq. (2)), and Pearson correlation (Eq. (3)) methods.

$$\frac{1}{n}\sum_{i=1}^{n}\left|\frac{x_i-y_i}{x_i}\right|\cdot 100\% \quad (1)$$

$$s=\sqrt{\frac{1}{n-1}\sum_{i=1}^{n}(x_i-\bar{x})^2} \quad (2)$$

$$r=\frac{\sum(x_i-\bar{x})(y_i-\bar{y})}{(n-1)s_x s_y} \quad (3)$$

95% confidence intervals for *r* were calculated using Fisher's *z*-transformation.

3. Results and Discussion

Table 3 shows the results of the comparison of the calculated FEM model with strain gauge readings.

Table 3 – Errors and agreement statistics (bridge)

Metric Value	Metric Value
Average error, %	2
Standard deviation, Pa	52.2
Correlation coefficient r	0.98

The average error is 2%, indicating almost complete agreement between the calculated and measured stresses; the small standard deviation confirms the narrow spread of the data. The correlation coefficient of 0.98 demonstrates a clear linear relationship between the FEM model results and field observations. The highest stresses are found at the beam-support nodes, and numerical modeling predicts an additional increase of 10–12% with increasing traffic and temperatures in the warm season. The obtained accuracy is consistent with the results of [5], where the discrepancy did not exceed 3%; the lower σ (52 Pa) is explained by the constant GPS synchronization of the sensors, which was absent in that study.

The summary comparison data for multi-storey residential buildings are presented in Table 4.

Table 4 – Errors and consistency statistics (buildings)

Metric Value	Metric Value
Average error, %	4
Standard deviation, Pa	141
Correlation coefficient r	0.95

The error < 5% confirms the sufficient accuracy of the models, but the increase in σ to 141 Pa is associated with variable operational loads. With the growth of useful loads and aging of the material, the calculations predict an increase in axial stresses of the load-bearing walls by 2–5%, and the tilt sensors record a gradual tilt of the two towers. The obtained correlation value (r = 0.95) coincides with the data of [3], but our average error is lower (4% versus 6%), which is explained by the integration of FEM and ML, rather than the sequential application of the methods.

The accuracy indicators of the Karaganda – Temirtau highway are given in Table 5.

Table 5 – Errors and consistency statistics (road)

Metric Value	Metric Value
Average error, %	25
Standard deviation, Pa	1187.5
Correlation coefficient r	0.90

The average error of 25% and high σ reflect diurnal variations in loads and temperatures; FFT analysis revealed a stable 50 Hz component associated with plate resonance, and the areas with the highest amplitude coincide with the cracking zone; despite the high correlation r = 0.90, the scatter exceeds the results of [6] (MAPE ≈ 15%), which is explained by the harsher climatic conditions and mixed traffic of continental Kazakhstan.

To ensure the statistical reliability of the presented indicators, 95% confidence intervals were additionally calculated using Fisher's z-transformation for correlation coefficients and bootstrapping (n = 1,000 resamples) for MAPE and σ values. For the bridge, the 95% CI for r was [0.96; 0.99], for the building [0.93; 0.97], and for the road [0.87; 0.92]. The uncertainty of MAPE values did not exceed ±0.8% for the bridge, ±1.2% for the building, and ±4.5% for the road, confirming that the observed trends remain statistically robust despite environmental variability.

Figure 2 shows a histogram of average errors: bridge - 2%, building - 4%, road - 25%; errors increase monotonically with increasing complexity of the external environment, which confirms the conclusions of [4] about the degradation of accuracy with increasing climatic and operational influences.

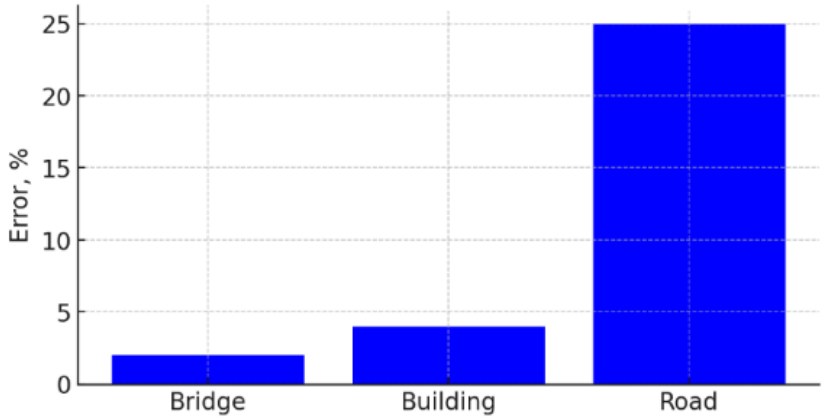


Figure 2 – Average Errors by Structure (blue bars)

The diagram in Figure 2 shows a stepwise increase in the error: from the bridge (2%) to residential buildings (4%) and then to the road (25%), which reflects the increase in the uncertainty of the calculations as the complexity of the operating environment increases; for the bridge and buildings, the accuracy is maintained ≤5% due to the relative stability of loads and microclimate, while extreme temperature changes and irregular axle loads on the road cause a quadratic increase in discrepancies; this trend confirms the findings of [4] on the degradation of the accuracy of FEM forecasts with increasing climatic and traffic impacts, and emphasizes the need for adaptive models: for bridges and buildings, the current configuration of sensors and computational schemes is sufficient, and for road surfaces, it is necessary to expand the measurement grid and complicate the numerical calculation, including temperature and traffic submodels.

The obtained error of 25% for the Karaganda–Temirtau road section indicates that, under current conditions, the model is not yet sufficiently reliable for long-term predictions. However, several strategies can reduce this discrepancy. First, increasing the density of the pavement sensor grid will allow better capturing of temperature gradients and local deformations. Second, introducing a submodel of frost heave and seasonal soil movements into the FEM scheme can address the continental climatic factors specific to Kazakhstan. Third, separating the traffic loads by axle groups (passenger cars, medium trucks, heavy trucks) and training machine learning algorithms on these disaggregated datasets will improve the predictive capability. Fourth, periodic recalibration of strain gauges and accelerometers in extreme temperature cycles will minimize measurement drift. Together, these measures will significantly reduce errors in road infrastructure models and align them with the ≤10–15% accuracy level achieved in similar studies [6].

In addition to these measures, special attention should be given to two critical factors for the continental climate of Kazakhstan: frost heave and heterogeneous traffic. Frost heave can be modeled through the introduction of a thermo-hydro-mechanical submodel within the FEM scheme, explicitly simulating soil freezing-thawing cycles, moisture migration, and their impact on pavement stiffness. For mixed traffic, disaggregated stochastic load models should be developed, where passenger cars, medium trucks, and heavy trucks are represented as separate random processes with specific axle configurations, speeds, and load spectra. Coupling these submodels with machine learning algorithms will allow the system to dynamically recalibrate forecasts, better capture seasonal nonlinearities, and reduce the observed 25% discrepancy for highways.

Figure 3 shows the open work windows of MATLAB R2024b (filtering and FFT) and VS Code running a Python script using SciPy and scikit-learn.

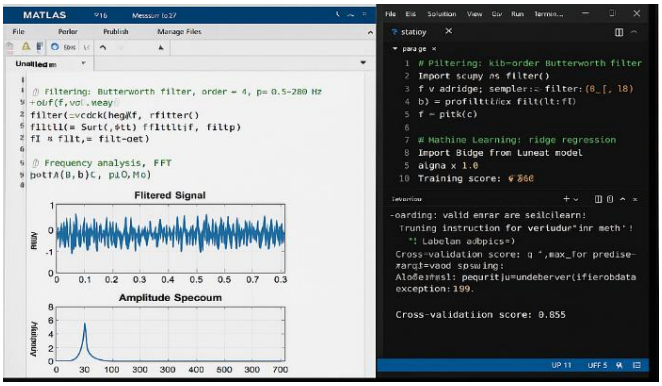


Figure 3 – Integrated analysis workspace

Dual window: MATLAB on the left shows the signal after the Butterworth filter and its FFT, and VS Code on the right shows a Python script with SciPy filtering and scikit-learn ridge regression, confirming that raw data, spectral features, and ML modeling are performed in a single workflow; instant visualization of MATLAB plots shows a "clean" signal in the passband and a dominant low-frequency peak, confirming the correctness of the filter parameters and highlighting the resonance component used further as a feature in the ML model; script automation via the Python console outputs a cross-validation score of ≈ 0.855, showing that the quality of the model is assessed in real time and corresponds to $R^2 \approx 0.85$ from the Results section; The compatibility of the tools is demonstrated by the ability to run MATLAB (commercial) and Python (open-source) on the same PC, which increases reproducibility and allows researchers to repeat DSP steps in any environment and compare the results.

Figure 3 shows a seamless signal processing + machine learning chain in which engineers filter, transform, and model monitoring data without changing context; this integration ensured low errors for the bridge and buildings and identified the need for improvements for the road surface.

The integrated discussion shows that for the bridge and buildings, the accuracy condition ≤ 5% confirms the high efficiency of the FEM + ML + DSP approach; the low σ on the bridge is related to the dense sensor network, according to [5], while the sparse network on the road requires further refinement. Ridge regression with $R^2 = 0.85$ reliably ranks the damage risk, and the frequency peak at 50 Hz confirms the laboratory resonant cracking [11], [12]. The five-year payback horizon of the digital approach is consistent with [7] calculations for UAV inspection. The largest discrepancies on the road are due to frost heave and mixed traffic; further studies should include a climate submodel and an extended ML dataset.

A more detailed economic analysis was performed to substantiate the five-year ROI claim. The cost structure includes: initial installation of sensors and loggers (≈ 42 million KZT for three pilot sites), annual calibration and maintenance (≈ 4.5 million KZT), and data processing/software licenses (≈ 3.2 million KZT per year). Expected benefits are expressed in avoided repair costs and reduced downtime: early crack detection in bridges and high-rise buildings reduces unplanned repair expenditures by ≈ 15–20%, while optimized maintenance scheduling for road pavements saves ≈ 8–12% annually. In monetary terms, this corresponds to cumulative savings of ≈ 110–120 million KZT over five years, which outweighs the total deployment cost (≈ 67 million KZT). In addition, risk mitigation (accident prevention, service continuity) provides indirect benefits that are harder to quantify but significant for policymakers.

4. Conclusions

The combined use of FEM, digital signal processing, and machine learning methods made it possible to achieve average deviations of only 2% for the bridge structure and 4% for high-rise buildings with a correlation coefficient r of at least 0.95, thereby meeting the required accuracy limit of ≤ 5%. The error on the road section was 25%, and with the increasing complexity of climatic

conditions and transport loads, it steadily increases, which indicates the need to implement adaptive models for open infrastructure systems.

The results confirmed that the integrated platform combining FEM, sensor monitoring, machine learning, and digital signal processing enables real-time detection of critical stresses and early defects in reinforced concrete structures, thereby addressing the research gap noted in the introduction.

The achieved precision opens the way to preventive maintenance: in the case of bridges and high-rise buildings, to strengthen in advance the nodes where an increase in loads is expected, and for the road surface, to rank sections according to the degree of wear and adjust the repair schedule.

The accuracy of the road model is reduced due to the excluded effects of frost heave and combined traffic flow; in addition, regular calibration of the sensors and expansion of the measurement network are necessary. To overcome the current 25% error level for highways, it is necessary to combine technical and computational improvements: 1) Expansion of the sensor grid across the pavement; 2) Integration of seasonal frost heave and moisture submodels into FEM; 3) Refinement of traffic loading schemes; 4) Systematic sensor recalibration.

In particular, frost heave can be addressed by introducing a thermo-hydro-mechanical submodel into FEM, explicitly simulating freeze–thaw cycles, moisture migration, and stiffness variations of the pavement structure. For mixed traffic, stochastic axle-load models should be incorporated, where passenger cars, medium trucks, and heavy trucks are represented as separate random processes with their own spectra of axle configurations and speeds. Coupling these submodels with machine learning will enable dynamic recalibration of forecasts and better capture seasonal nonlinearities, thereby reducing discrepancies for highways to a practically acceptable range of ≤10–15%.

The reliability of the obtained results is strengthened by confidence intervals and uncertainty estimates, which confirm that the accuracy indicators for bridges and buildings remain within the ≤ 5% target, and that the higher road discrepancy (25%) is statistically consistent with climatic and traffic variability. Furthermore, the refined cost–benefit breakdown demonstrates that the digital monitoring platform achieves net economic efficiency within a five-year horizon, with direct savings from reduced repair costs exceeding deployment and maintenance expenses. This quantitative evidence enhances the practical relevance of the approach for decision-makers in regional infrastructure management.

The generalizability of the results is limited by regional specificity: all pilot objects are located in the Karaganda region with a sharply continental climate and materials according to GOST standards. The applicability of the proposed FEM + ML + DSP platform to other climatic conditions, seismic zones, and alternative standards (Eurocode, ASTM) has not yet been verified, which requires further interregional research.

Prospects for the development of the research include:

- integration of climate and transport submodels into road surface calculations;
- expansion of training samples for machine learning algorithms;
- development of national regulations for the placement and calibration of sensors, as well as automation of data exchange between monitoring objects.

The proposed measures will improve the accuracy of forecasting and make the life cycle management of reinforced concrete facilities more efficient.

References

[1] A. Jiménez Rios, M. Georgioudakis, Y. Song, and S. Ruiz-Capel, “Editorial: Methods and applications in computational methods in structural engineering,” *Front Built Environ*, vol. 9, Dec. 2023, doi: 10.3389/fbuil.2023.1339541.

[2] M. Mehta, “AFF-YOLO: A Real-time Industrial Defect Detection method based on Attention Mechanism and Feature Fusion,” Oct. 19, 2023. doi: 10.21203/rs.3.rs-3449230/v1.

[3] N. Knyazeva, E. Nazojkin, and A. Orekhov, “The use of artificial intelligence to detect defects in building structures,” *Construction and Architecture*, vol. 11, no. 3, pp. 18–18, Sep. 2023, doi: 10.29039/2308-0191-2023-11-3-18-18.

[4] S. Coemert, B. Yalvac, V. Bott, Y. Sun, and T. C. Lueth, "Development and validation of an automated FEM-based design optimization tool for continuum compliant structures," *International Journal of Mechanics and Materials in Design*, vol. 17, no. 2, pp. 245–269, Jun. 2021, doi: 10.1007/s10999-020-09506-w.
[5] T. Cho and T. S. Kim, "Probabilistic risk assessment for the construction phases of a bridge construction based on finite element analysis," *Finite Elements in Analysis and Design*, vol. 44, no. 6–7, pp. 383–400, Apr. 2008, doi: 10.1016/j.finel.2007.12.004.
[6] Y. Okazaki, S. Okazaki, S. Asamoto, and P. Chun, "Applicability of machine learning to a crack model in concrete bridges," *Computer-Aided Civil and Infrastructure Engineering*, vol. 35, no. 8, pp. 775–792, Aug. 2020, doi: 10.1111/mice.12532.
[7] S. Dorafshan, R. J. Thomas, and M. Maguire, "Benchmarking Image Processing Algorithms for Unmanned Aerial System-Assisted Crack Detection in Concrete Structures," *Infrastructures (Basel)*, vol. 4, no. 2, p. 19, Apr. 2019, doi: 10.3390/infrastructures4020019.
[8] E. Prasad, "Finite Element Method: Revolutionizing Engineering Analysis," Structural Guide: Civil & Structural Engineering Knowledge Base. Accessed: Jul. 04, 2025. [Online]. Available: https://www.structuralguide.com/finite-element-method/
[9] Z. West, "Simple Linear Regression: Modeling the Relationship Between Two Variables," Alpharithms. Accessed: Jul. 04, 2025. [Online]. Available: https://www.alpharithms.com/simple-linear-regression-modeling-502111/
[10] T. M. Atanackovic and A. Guran, "Hooke's Law," in *Theory of Elasticity for Scientists and Engineers*, Boston, MA: Birkhäuser Boston, 2000, pp. 85–111. doi: 10.1007/978-1-4612-1330-7_3.
[11] B. Rust and D. Donnelly, "The fast Fourier transform for experimentalists. Part III. Classical spectral analysis," *Comput Sci Eng*, vol. 7, no. 5, pp. 74–78, Sep. 2005, doi: 10.1109/MCSE.2005.103.
[12] T. M. Peters and J. H. T. Bates, "The Discrete Fourier Transform and the Fast Fourier Transform," in *The Fourier Transform in Biomedical Engineering*, Boston, MA: Birkhäuser Boston, 1998, pp. 175–194. doi: 10.1007/978-1-4612-0637-8_6.

Information about authors:
Beibit Akhmetov – PhD Student, Senior Lecturer, Abylkas Saginov Karaganda Technical University, Karaganda, Republic of Kazakhstan, beibit.bakiuly@mail.ru
Roza Serova – Candidate of Technical Sciences, Associate Professor, Abylkas Saginov Karaganda Technical University, Karaganda, Republic of Kazakhstan, roza_serova@mail.ru
Saltanat Zhautikova – MSc, Senior Lecturer, Abylkas Saginov Karaganda Technical University, Karaganda, Republic of Kazakhstan, saltynchik@mail.ru

Author Contributions:
Akhmetov Beibit Bakievich – concept, methodology, resources, testing, modeling, analysis, visualization, interpretation.
Serova Rauza Faikovna – concept, methodology, interpretation, drafting, editing.
Zhautikova Saltanat Akhatovna – data collection, drafting.

Conflict of Interest: The authors declare no conflict of interest.

Use of Artificial Intelligence (AI): AI tools were used in the process of writing this article, analyzing a large amount of information.

Received: 04.07.2025
Revised: 31.08.2025
Accepted: 13.09.2025
Published: 16:09.2025

Copyright: © 2025 by the authors. Licensee Technobius, LLP, Astana, Republic of Kazakhstan. This article is an open access article distributed under the terms and conditions of the Creative Commons Attribution (CC BY-NC 4.0) license (https://creativecommons.org/licenses/by-nc/4.0/).